Kinetic Analysis of the Reaction between Electrogenerated Superoxide and Carbon Dioxide in the Room Temperature Ionic Liquids 1-Ethyl-3-methylimidazolium Bis(trifluoromethylsulfonyl)imide and Hexyltriethylammonium Bis(trifluoromethylsulfonyl)imide

Marisa C. Buzzeo,[†] Oleksiy V. Klymenko,[†] Jay D. Wadhawan,[†] Christopher Hardacre,[‡] Kenneth R. Seddon,[‡] and Richard G. Compton*[,†]

Physical and Theoretical Chemistry Laboratory, University of Oxford, South Parks Road, Oxford OX1 3QZ, United Kingdom, and School of Chemistry, The Queen's University of Belfast, Belfast, Northern Ireland BT9 5AG, United Kingdom

Received: September 30, 2003

The reduction of oxygen in the presence of carbon dioxide has been investigated by cyclic voltammetry at a gold microdisk electrode in the two room-temperature ionic liquids 1-ethyl-3-methylimidazolium bis(trifluoromethylsulfonyl)imide ([EMIM][$N(Tf)_2$]) and hexyltriethylammonium bis(trifluoromethylsulfonyl)imide ([N_{6222}][$N(Tf)_2$]). With increasing levels of CO_2, cyclic voltammetry shows an increase in the reductive wave and diminishing of the oxidative wave, indicating that the generated superoxide readily reacts with carbon dioxide. The kinetics of this reaction are investigated in both ionic liquids. The reaction was found to proceed via a DISP1 type mechanism in [EMIM][$N(Tf)_2$], with an overall second-order rate constant of $1.4 \pm 0.4 \times 10^3$ M^{-1} s^{-1}. An ECE or DISP1 mechanism was determined to be the most likely pathway for the reaction in [N_{6222}][$N(Tf)_2$], with an overall second-order rate constant of $1.72 \pm 0.45 \times 10^3$ M^{-1} s^{-1}.

Introduction

The chemistry and reactivity of superoxide has been studied in a variety of systems.[1−10] The superoxide species that is electrochemically generated from the one electron reduction of oxygen

$$O_2 + e^- \rightarrow O_2^{-\bullet} \quad (1)$$

can act as a strong base, free radical, or nucleophile and readily disproportionates in water

$$2O_2^{-\bullet} + H_2O \rightarrow O_2 + HOO^- + HO^- \quad (2)$$

For this reason, aprotic solvents, such as acetonitrile (MeCN) and dimethyl sulfoxide (DMSO), are most commonly employed for the reduction of oxygen in order to produce stable anions. Sawyer and Roberts[2] studied the electrochemistry of superoxide in DMSO at platinum, gold, and mercury electrodes and reported values for the diffusion coefficients of oxygen and superoxide in 0.1 M $(Et)_4NClO_4$-DMSO solution ($D_{O_2} = 3.23 \times 10^{-9}$ m^2 s^{-1} and $D_{O_2^{-\bullet}} = 1.08 \times 10^{-9}$ m^2 s^{-1}). When generated in such aprotic systems, the reactivity of superoxide with a variety of chemical species can be studied. Superoxide has been shown to react with alkyl halides to form peroxide radicals via nucleophilic displacement of the halide,[11] to convert primary alcohols to carboxylic acids,[12] and to convert secondary nitroalkanes and alcohols to the corresponding ketones.[13,14]

In the presence of carbon dioxide, superoxide nucleophilically attacks the carbon in CO_2 to give $CO_4^{-\bullet}$, which subsequently reacts with another molecule of CO_2 to ultimately form the peroxodicarbonate ion, $C_2O_6^{2-}$, in an overall two electron process per molecule superoxide. Roberts et al.[15] have studied this reaction in aprotic media and analyzed the reaction kinetics by the rotating ring-disk voltammetric method. The reaction was found to be first order with respect to both superoxide and carbon dioxide and second-order overall. Casadei and co-workers[16−18] have studied the activation of CO_2 by $O_2^{-\bullet}$ and have shown that the electrogenerated carboxylating reagent will convert primary and secondary alcohols bearing a leaving group in the α or β position to the corresponding cyclic carbonates.

Development of a sensor that is capable of detecting carbon dioxide in a reliable and inexpensive manner is of significant importance to both the medical profession and socially responsible industries, such as breweries, fermentation industries, and fabrication plants.[19,20] Over the past two decades, advances have been made in the ability to detect oxygen and carbon dioxide in the presence of one another. As oxygen is more easily electrochemically reduced than carbon dioxide,[5] the simultaneous amperometric detection of oxygen and carbon dioxide becomes complicated since the generated superoxide will readily attack carbon dioxide. In 1982, Albery and Barron[5] reported a new metallised membrane electrode which allowed for the simultaneous determination of CO_2 and O_2, whereby O_2 is effectively filtered through aqueous solvent prior to detection of CO_2. The observed signal showed good linearity with concentration for both O_2 and CO_2. Based on earlier work done by Albery[5,21] and Hahn,[8,22] Zhou and co-workers[23,24] developed a modulated potential pulse-amperometry/coulometry method, which employed computer-controlled fast modulated potential techniques to simultaneously detect these gases at microelectrodes. Wadhawan et al.[9,10] reported the simultaneous detection of oxygen and carbon dioxide at a gold microdisk electrode in

* To whom correspondence should be addressed. Tel: 01865 275413. Fax: 01865 275410. Email: Richard.Compton@chemistry.ox.ac.uk.
[†] University of Oxford.
[‡] The Queen's University of Belfast.

10.1021/jp031121z CCC: $27.50
Published on Web 02/27/2004

a series of aprotic solvents and have analyzed the kinetics of the reaction between the electrogenerated superoxide and carbon dioxide.

In addition to conventional aprotic solvents, the investigation of gas dissolution and detection has been recently explored in room-temperature ionic liquids (RTILs).[25−35] The intrinsic properties of RTILs, including negligible volatility and high thermal stability,[36−38] make them a desirable alternate to traditional media for a variety of chemical processes, including the electrochemical pursuit of gas detection. Anthony et al.[29,32] have studied the solubilities and thermodynamic properties of several different gases in the ionic liquid 1-butyl-3-methylimidazolium hexafluorophosphate, [BMIM][PF_6], whereas Husson-Borg et al.[35] have recently reported solubility data for O_2 and CO_2 in the tetrafluoroborate salt, [BMIM][BF_4]. The one electron reduction of oxygen in room-temperature imidazolium chloride-aluminum chloride molten salts was first reported by Carter et al.[25] Contamination of the molten salts by trace amounts of water, however, prevented formation of stable superoxide ions. AlNashef et al.[30] have since given evidence of stable electrochemically generated superoxide ions in [BMIM]-[PF_6] and subsequently reported preliminary evidence of the reduction of oxygen in the presence of carbon dioxide in the same ionic liquid.[33] An increase in the reductive current and decrease in the oxidative back peak was observed and the generated carboxylating reagent is thought to have potential applications in organic synthesis and green chemistry.

In this paper, we report the reduction of oxygen in the presence of carbon dioxide in the RTILs 1-ethyl-3-methylimidazolium bis(trifluoromethylsulfonyl)imide ([EMIM][$N(Tf)_2$]) and hexyltriethylammonium bis(trifluoromethylsulfonyl)imide ([N_{6222}][$N(Tf)_2$]) as detected by cyclic voltammetry (CV) at a gold microdisk electrode. The kinetics of the reaction between superoxide and carbon dioxide are analyzed in both ionic liquids, and despite significantly different viscosities, the reaction between superoxide and carbon dioxide are found to proceed via similar a mechanism in both [EMIM][$N(Tf)_2$] and [N_{6222}]-[$N(Tf)_2$] cf. aprotic organic solvents.

Theory

Transients. To determine the concentration and the diffusion coefficient of oxygen and carbon dioxide in the ionic liquids, chronoamperometric experiments were performed at the Au microdisk electrode. Theoretical transients were then calculated using the equation derived by Aoki[39]

$$i = 4nFr_e D_0 c_0(\tau) \tag{3}$$

where i is the time-dependent current, n is the number of electrons transferred, F is the Faraday constant (96 485 C mol^{-1}), r_e is the radius of the microdisk, D_0 is the diffusion coefficient of the electroactive species, c_0 is the bulk concentration of the electroactive species and τ is a dimensionless parameter defined as $\tau = 4D_0t/r_e^2$.[39] The exact form of the function $f(\tau)$ depends on the value of τ. At short times ($\tau < 1.44$)

$$f(\tau) = 0.88623\tau^{-1/2} + 0.78540 + 0.094\tau^{1/2} \tag{4}$$

At long times ($\tau > 0.82$)

$$f(\tau) = 1 + 0.71835\tau^{-1/2} + 0.05626\tau^{-3/2} - 0.00646\tau^{-5/2} \tag{5}$$

These two functions overlap in the range ($0.82 < \tau < 1.44$).[40] Using 1×10^{-10} m^2 s^{-1} as an estimate for the value of the diffusion coefficient of oxygen in an ionic liquid, τ was calculated to be 6.9 at $t = 0.5$ s. Equation 5 was therefore used to generate theoretical transients using a nonlinear curve fitting program available in Origin 6.0 (Microcal Software, Inc.). Having specified the radius of the microdisk, the computer software optimized the fit between the experimental and theoretical transients by varying the values of the diffusion coefficient and concentration of the electroactive species. The accuracy of these values was then verified using a computer program designed to simulate cyclic voltammograms, as described in the following section.

Simulation of Cyclic Voltammograms. Let us consider the problem of cyclic voltammetry at a microdisk electrode for the reduction of oxygen in the presence of carbon dioxide (see Scheme 6). Based on previous work,[15,21,41] the reaction mechanism can be symbolically written as

$$\begin{aligned} A + e^- &\rightleftharpoons B \\ B + C &\xrightarrow{k_1} D \\ D + C &\xrightarrow{k_2} E \\ E + B &\xrightarrow{k_2} F + A \end{aligned} \tag{6}$$

where $A = O_2$, $B = O_2^{-\bullet}$, $C = CO_2$, $D = CO_4^{-\bullet}$, $E = C_2O_6^{-\bullet}$, $F = C_2O_6^{2-}$. We shall refer to it as ECCC reaction mechanism in the following.

The time dependent equations describing the mass transport of all of the species to a microdisk electrode of radius r_d written in cylindrical coordinates are

$$\begin{aligned} \frac{\partial[A]}{\partial t} &= D_A\nabla^2[A] + k_3[B][E] \\ \frac{\partial[B]}{\partial t} &= D_B\nabla^2[B] - k_1[B][C] - k_3[B][E] \\ \frac{\partial[C]}{\partial t} &= D_C\nabla^2[C] - k_1[B][C] - k_2[C][D] \\ \frac{\partial[D]}{\partial t} &= D_D\nabla^2[D] + k_1[B][C] - k_2[C][D] \\ \frac{\partial[E]}{\partial t} &= D_E\nabla^2[E] + k_2[C][D] - k_3[B][E] \end{aligned} \tag{7}$$

where D_A, D_B, ... are the diffusion coefficients of species A, B, ...; $\nabla^2 = (\partial^2/\partial r^2) + (1/r)(\partial/\partial r) + (\partial^2/\partial z^2)$ is the Laplacian in the cylindrical coordinates, in which r represents the radial coordinate and z the coordinate normal to the surface of the disk.

The initial conditions ($t = 0$) for the concentrations of all of the species taking part in the reaction mechanism (6) are

$$[A] = [A]_{bulk}; \quad [B] = 0; \quad [C] = [C]_{bulk}; \quad [D] = 0; \quad [E] = 0 \tag{8}$$

and the boundary conditions completing the mathematical model are presented in the Table 1, where k_f and k_b denote forward and reverse rate constants for the reduction step in the kinetic

TABLE 1: Boundary Conditions

boundary region	equations
$z = 0,\ 0 \le r \le r_d$	$D_A\left.\frac{\partial[A]}{\partial z}\right\|_{z=0} = (k_f'[A] - k_b'[B])_{z=0};\ D_B\left.\frac{\partial[B]}{\partial z}\right\|_{z=0} = -D_A\left.\frac{\partial[A]}{\partial z}\right\|_{z=0}$
	$\left.\frac{\partial[C]}{\partial z}\right\|_{z=0} = \left.\frac{\partial[D]}{\partial z}\right\|_{z=0} = \left.\frac{\partial[E]}{\partial z}\right\|_{z=0} = 0$
$z = 0,\ r > r_d$	$\left.\frac{\partial[A]}{\partial z}\right\|_{z=0} = \left.\frac{\partial[B]}{\partial z}\right\|_{z=0} = \left.\frac{\partial[C]}{\partial z}\right\|_{z=0} = \left.\frac{\partial[D]}{\partial z}\right\|_{z=0} = \left.\frac{\partial[E]}{\partial z}\right\|_{z=0} = 0$
all $z,\ r = 0$	$\left.\frac{\partial[A]}{\partial r}\right\|_{r=0} = \left.\frac{\partial[B]}{\partial r}\right\|_{r=0} = \left.\frac{\partial[C]}{\partial r}\right\|_{r=0} = \left.\frac{\partial[D]}{\partial r}\right\|_{r=0} = \left.\frac{\partial[E]}{\partial r}\right\|_{r=0} = 0$
$z,\ r \to \infty$	$[A] \to [A]_{bulk};\ [A] \to [A]_{bulk};\ [C] \to [A]_{bulk};\ [D] \to 0;\ [E] \to 0$

mechanism 1:

$$k_f = k_0 \exp\left(-\frac{\alpha F}{RT}(E - E^0)\right)$$

$$k_b = k_0 \exp\left(\frac{(1-\alpha)F}{RT}(E - E^0)\right) \qquad (9)$$

where k_0 is the standard heterogeneous rate constant for the *A*/*B* couple, α is the transfer coefficient, and $E°$ is the formal potential.

The current flowing at the electrode surface was calculated using the following expression:

$$i = -2\pi F D_A \int_0^{r_d} \left.\frac{\partial[A]}{\partial z}\right|_{z=0} r\, dr \qquad (10)$$

The coordinate transformation developed by Amatore and Fosset[42] was used to map an infinite area $[0,\infty) \times [0,\infty)$ in the cylindrical coordinates r, z onto a closed square $[0,1] \times [0,1]$ in the transformed θ,Γ space:

$$R = \frac{\sqrt{1-\theta^2}}{\cos\left(\frac{\pi}{2}\Gamma\right)};\quad Z = \theta \tan\left(\frac{\pi}{2}\Gamma\right) \qquad (11)$$

where $R = (r/r_d)$ and $Z = (z/r_d)$. This transformation effectively removes the edge singularity arising from the discontinuous boundary conditions and improves simulation efficiency due to the fewer number of the mesh nodes required to obtain the desired level of accuracy. It is perfectly suited for simulation of steady-state conditions at a microdisk electrode and is nearly-optimal for slow scan rate voltammetry simulations, which are considered here.

The alternating direction implicit (ADI) method[43−45] was used to solve the mass transport equations (7) in the two-dimensional domain. Newton's method[46] was used to solve systems of nonlinear algebraic equations arising from the discretisation of the partial differential equations (7). The generalized Thomas algorithm[47] for banded matrixes was used to solve linear systems.

All of the programs for the simulations were written in Delphi 6 Professional Edition (Borland Software Corporation, Scotts Valley, California) and executed on a PC with Pentium 4 2GHz processor and 1 GB of RAM.

The convergence properties of the simulation algorithm for the ECCC reaction were tested in a way similar to that described previously.[48] Both the forward and the back peak convergence tests were performed in order to ensure that the solution satisfies the accuracy requirements along the whole voltammogram, where the accuracy along the back scan depends on the ratio of the diffusion coefficients of A and B, as has been shown earlier.[49] Figure 1 shows the convergence for the back peak. The figure demonstrates the log−log plot of the relative error in the current $|i - i_{lim}|/i_{lim}$ versus the grid step size $h = 1/N\theta = 1/N\Gamma$. The rate of convergence was found from Figure 1 to be better than of the order $O(h^{0.84})$. The grid of the size $300 \times 300 \times 2000$ ($N\theta \times N\Gamma \times NT$) was found to be necessary to achieve convergence of the back peak current of about 1%. Such a high number of nodes needed to obtain accurate results can be explained by a large difference in the diffusion coefficients of the reacting species and hence different diffusion regimes for the neutral and charged species. However, a grid of this size was used only for obtaining theoretical results and for final stages of the voltammogram fitting since the simulation with this size grid requires approximately 30 min of CPU time due to the nonlinearity of the system of partial differential equations (7).

Theoretical Results. To check the mathematical model (7), (8), (Table 1) and the computer program written to solve it, we investigated two limiting cases for the linear sweep steady-state voltammetry (slow voltage scan rate) for the reaction mechanism of interest. The first limiting case corresponds to the absence of homogeneous kinetics in the mechanism, which is achieved by setting $k_1 = 0$. Under these conditions, the simulation results must be the same as those for a single electron transfer reaction. To test the results for this case, we simulated a linear sweep voltammogram with a slow scan rate to obtain a steady-state response. The results of this simulation were then compared with the limiting current expected from analytical theory and published independently simulated results for a simple E reaction.[44] Figure 2a shows this comparison where the solid line represents the simulated linear sweep voltammogram for the ECCC mechanism with $k_1 = 0$ normalized with respect to the

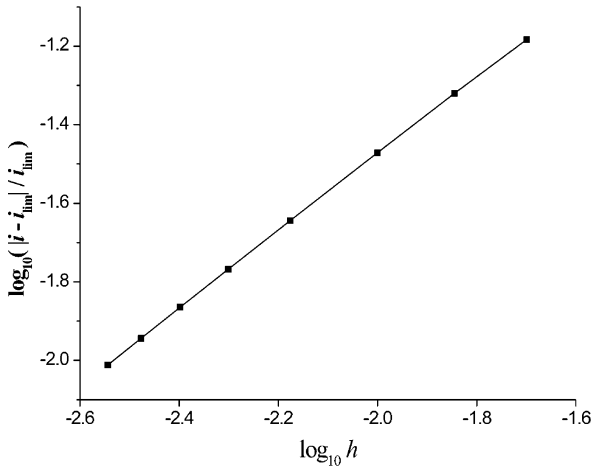

Figure 1. Convergence plot for the back peak current valid for the following parameter values: $[A]_{bulk} = [C]_{bulk} = 10^{-3}$ M, $D_A = D_C = 1.5 \times 10^{-6}$ cm^2 s^{-1}, $D_B = D_D = D_E = 2 \times 10^{-8}$ cm^2 s^{-1}, $k_0 \le 1$ cm s^{-1}, $\alpha = 0.5$, $r_d = 5$ μm, $0 \le k_i$/cm^3 mol^{-1} s^{-1} $\le 10^{10}$, $i = 1$, 2, and 3.

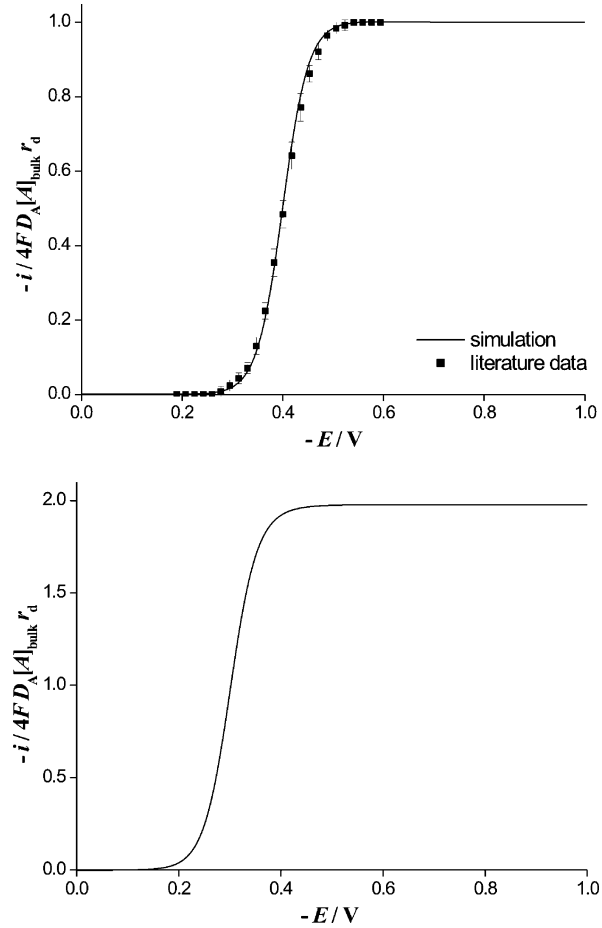

Figure 2. Linear sweep voltammograms for the two limiting cases simulated for the parameter values $[A]_{bulk} = 10^{-3}$ M, $[C]_{bulk} = 10^{-2}$ M, $D_A = D_B = 1 \times 10^{-6}$ cm^2 s^{-1}, $D_C = 5 \times 10^{-6}$ cm^2 s^{-1}, $D_D = D_E = 1 \times 10^{-7}$ cm^2 s^{-1}, $k_0 = 1$ cm s^{-1}, $\alpha = 0.5$, $r_d = 5$ μm, $E° = -0.4$ V. (a) E-reaction limit, $k_i = 0$, $i = 1$, 2, and 3; (b) fast heterogeneous kinetics limit, $k_1 = 10^{13}$ cm^3 mol^{-1} s^{-1}, $k_2 = k_3 = 10^{16}$ cm^3 mol^{-1} s^{-1}.

predicted limiting current[50] and the dots correspond to the literature data for a simple E reaction.[44] The error bars shown for the literature data points reflect inaccuracies in reading the data values from the published paper. The agreement of these voltammograms suggests that the first E step in the mechanism is simulated correctly.

The second pronounced limiting case corresponds to fast homogeneous kinetics and an excess of species C. A 2-fold increase in the limiting current is expected compared to that of a one-electron process as a result of the regeneration of species A in the last step of the reaction mechanism. Figure 2b demonstrates the simulated voltammogram normalized to the theoretical limiting current for one-electron transferred.[50] The simulation parameters are given in the figure legend. As can be seen, the simulated current displays the expected behavior. This demonstrates the consistency of the proposed simulation procedure.

Experimental Section

Chemical Reagents. RTILs 1-ethyl-3-methylimidazolium bis(trifluoromethylsulfonyl)imide, [EMIM][N(Tf)$_2$], and hexyltriethylammonium bis(trifluoromethylsulfonyl)imide, [N_{6222}][N(Tf)$_2$], were synthesized from the corresponding bromide or chloride salt via a metathesis reaction in aqueous lithium, as described by Bonhôte et al.[26] Ferrocene (Aldrich), tetrabutylammonium perchlorate (TBAP, Fluka), and acetonitrile (Fisher Scientific) were used directly without further purification. Impurity free oxygen, nitrogen, (BOC, Guildford, Surrey, U.K.), and carbon dioxide (Messer, Cedar House, Surrey, U.K.) were used for electrochemical experiments as described below.

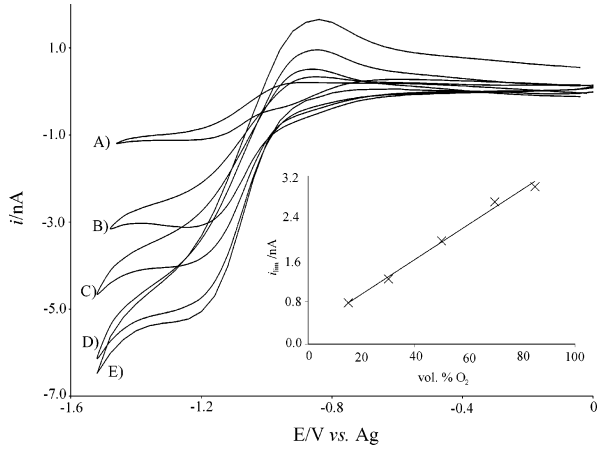

Figure 3. Cyclic voltammograms (1 V s^{-1} scan rate) for the reduction of O_2 in [EMIM][N(Tf)$_2$] at a 10.8 μm Au microdisk electrode at varying vol. % O_2. (A) 15, (B) 30, (C) 50, (D) 70, and (E) 85 vol. % O_2. The inset shows a plot of limiting current *vs.* vol. % O_2.

Instrumentation. A commercial potentiostat, PGSTAT 20 (Eco Chemie Utrecht, Netherlands) was used for the electrochemical experiments in conjunction with a Pentium-based PC. The 10 μm Au (diameter) microdisk working electrode (Cypress Systems, Kansas) comprised a Au wire sealed in borosilicate glass which was carefully polished using a 1.0 μm alumina slurry (Kermet, Kent, U.K.), followed by a 0.3 μm alumina suspension (Buehler, Lake Bluff, IL). The electrode was then polished on a clean, damp cloth (Microcloth, Buehler), immersed in 10% nitric acid solution to remove any adventitious adsorbates and then rinsed with acetonitrile. The diameter of the microdisk electrode was calibrated electrochemically using 2 mM ferrocene in 0.1 M TBAP/acetonitrile, using a value for the diffusion coefficient of 2.3×10^{-5} cm^2 s^{-1} at 20 °C.[51]

A short piece (2 cm long) of heat-shrink tubing was fitted around the glass surrounding the working electrode to provide a casing to which ~20 μL of ionic liquid was delivered by micropipet. For those electrochemical experiments performed in [EMIM][N(Tf)$_2$], the outer circumference of the glass was coated with silver-loaded conducting paint (RS Chemicals), which served as a counter/reference electrode. For those conducted in [N_{6222}][N(Tf)$_2$], a silver wire was secured around the heat-shrink tubing, acting as a counter/reference electrode. All experiments were carried out in an electrochemical cell designed to sustain vacuum conditions at a temperature of 20 ± 3 °C, identical to that reported previously.[49]

Prior to the addition of gases, the sample of ionic liquid was placed under vacuum (Edwards High Vacuum Pump, Model ES 50) until the baseline showed little trace of atmospheric oxygen (typically ~90 min). Oxygen, carbon dioxide, and nitrogen were introduced to the electrochemical cell in the desired ratios using a Wösthoff triple gas-mixing pump (Bochum, Germany), accurate to ±1%. Gas mixtures were passed through the cell for at least 30 min before final measurements were taken to ensure that equilibration of the gases and the ionic liquid had been established.

Results and Discussion

Reduction of Oxygen in [EMIM][N(Tf$_2$)]. Figure 3 shows typical cyclic voltammograms (scan rate 1 V s^{-1}) for the one

electron reduction of oxygen at a 10.8 μm (diameter) Au microdisk electrode in [EMIM][$N(Tf)_2$] for increasing volume percent of oxygen from 15% to 85%, with nitrogen making up the remainder of the mixture. The half-wave potential occurs at −0.98 V vs Ag and the plot of current versus percent volume of O_2 (see inset, Figure 3) shows good linearity for the signal observed for the one electron reduction. The generated superoxide is stable and the reduction of oxygen is reversible, as proven by the presence of the back peak corresponding to the oxidation of superoxide back to oxygen. The asymmetry of the forward and reverse peaks reflects the difference in rate of diffusion of oxygen versus superoxide in the ionic liquid.[49]

The concentration and diffusion coefficient of oxygen in the ionic liquid were determined from a combination of potential chronoamperometric measurements and theoretical simulations as previously reported.[49] The concentration of oxygen in a saturated sample of [EMIM][$N(Tf)_2$] was found to be 3.9 mM, giving a Henry's Law constant of 3.9 mM atm^{-1}. With the value of D_{O_2} obtained from fitting of the transients as an initial approximation, D_{O_2} and $D_{O_2^{-\bullet}}$ were adjusted to give the best fit between experimental and theoretical voltammograms over a range of concentrations of O_2 using the simulation program described above. The average value of D_{O_2} was found to be 7.3 $\times$ 10^{-10} m^2 s^{-1}, compared to a value of 2.2 $\times$ 10^{-10} m^2 s^{-1} reported for [BMIM][PF_6],[30] whereas the average value of $D_{O_2^{-\bullet}}$ was 2.7 $\times$ 10^{-10} m^2 s^{-1}.

We now turn to the voltammetric investigation of the reduction of O_2 in the presence of CO_2 in [EMIM][$N(Tf)_2$]. The kinetics of the reaction between superoxide and carbon dioxide are subsequently analyzed.

Reduction of Oxygen in the Presence of Carbon Dioxide in [EMIM][$N(Tf)_2$]; Kinetic Analysis of the Reaction Between Superoxide and Carbon Dioxide. The reduction of oxygen in the presence of carbon dioxide was investigated by cyclic voltammetry in [EMIM][$N(Tf)_2$] at a gold microdisk electrode. As previously reported,[9,15,21] the mechanism for the reaction of superoxide with carbon dioxide is thought to proceed as follows:

$$2O_2 + 2e^- \rightleftharpoons 2O_2^{-\bullet} \quad (12)$$

$$O_2^{-\bullet} + CO_2 \rightarrow CO_4^{-\bullet} \quad (13)$$

$$CO_4^{-\bullet} + CO_2 \rightarrow C_2O_6^{-\bullet} \quad (14)$$

$$C_2O_6^{-\bullet} + O_2^{-\bullet} \rightarrow C_2O_6^{2-} + O_2 \quad (15)$$

$$\text{Overall: } O_2 + 2CO_2 + 2e^- \rightarrow C_2O_6^{2-} \quad (16)$$

Figure 4 shows the cyclic voltammograms (scan rate 1 V s^{-1}) for the reduction of oxygen in the presence of CO_2 at a 10.8 μm (diameter) Au microdisk electrode in [EMIM][$N(Tf)_2$], whereas Figure 5 shows the comparison of voltammograms (scan rate 1 V s^{-1}) obtained for the reduction of oxygen in a 50% O_2/50% N_2 gas mixture and those obtained in a 50% O_2/50% CO_2 mixture. As can be seen, the reductive wave increases and the oxidative wave disappears with the addition of carbon dioxide, suggesting that the electrogenerated superoxide is "titrated" by carbon dioxide.

A series of experiments were then performed in order to investigate the mechanism and kinetics of this reaction between the superoxide and carbon dioxide in [EMIM][$N(Tf)_2$]. The volume percentage of oxygen was held constant while the amount of carbon dioxide introduced to the cell was varied over

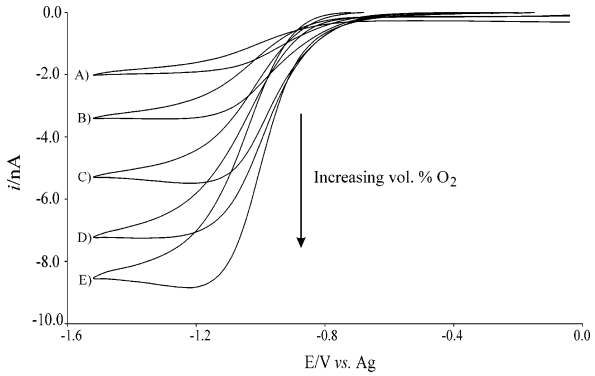

Figure 4. Cyclic voltammograms (1 V s^{-1} scan rate) for the reduction of oxygen in the presence of CO_2 at a 10.8 μm (diameter) Au microdisk electrode in [EMIM][$N(Tf)_2$]. (A) 15%O_2/85%CO_2, (B) 30%O_2/70%CO_2, (C) 50%O_2/50%CO_2, (D) 70%O_2/30%CO_2, (E) 85%O_2/15%CO_2.

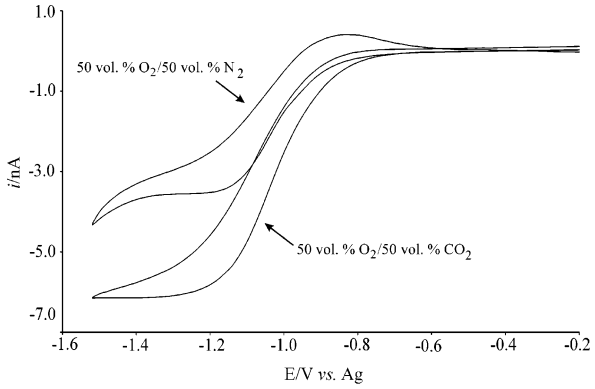

Figure 5. Cyclic voltammograms (1 V s^{-1} scan rate) for the reduction of oxygen in a 50% O_2/50% N_2 gas mixture and in a 50% O_2/50% CO_2 mixture.

a range of 2−16 vol %. Nitrogen made up the remainder of all gas mixtures. In the presence of 2 vol. % carbon dioxide, the reductive current increases suitably in comparison to that observed for pure O_2, but a doubling effect is not seen. If the mechanism were to switch from the one electron reduction of oxygen

$$O_2 + e^- \rightarrow O_2^{-\bullet} \quad (17)$$

to the overall two electron process for the reaction of superoxide with carbon dioxide

$$O_2 + 2CO_2 + 2e^- \rightarrow C_2O_6^{2-} \quad (18)$$

the reductive current is expected to double.[5,9,10,15] While the current did increase with the addition of carbon dioxide, the maximum increase was by a factor of 1.6. This observation likely results from slower reaction kinetics in the ionic liquid medium cf. in conventional aprotic solvents (see below).[9,41]

The mechanism of the nucleophilic addition of superoxide to carbon dioxide involves the heterogeneous transfer of an electron to dioxygen at the gold working electrode surface, followed by two homogeneous chemical steps and then either further electron transfer or a disproportionation step. A mixture of ECE, DISP1, and DISP2 processes have been used to best

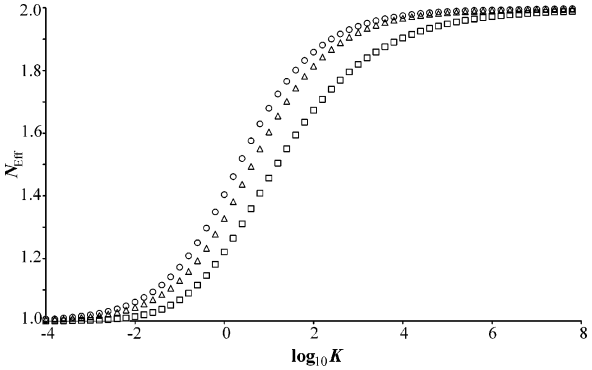

Figure 6. Working curves for ECE (○), DISP1 (△), and DISP2 (□) processes at microdisk electrodes.

describe this mechanism:[9,10]

ECE:

$$O_2 + e^- \rightarrow O_2^{-\bullet}$$

$$O_2^{-\bullet} + CO_2 \xrightarrow{k,\text{slow}} CO_4^{-\bullet}$$

$$CO_4^{-\bullet} + CO_2 \xrightarrow{\text{fast}} C_2O_6^{-\bullet}$$

$$C_2O_6^{-\bullet} + e^- \rightarrow C_2O_6^{2-}$$

DISP1:

$$2O_2 + 2e^- \rightarrow 2O_2^{-\bullet}$$

$$O_2^{-\bullet} + CO_2 \xrightarrow{k,\text{slow}} CO_4^{-\bullet}$$

$$CO_4^{-\bullet} + CO_2 \rightarrow C_2O_6^{-\bullet}$$

$$C_2O_6^{-\bullet} + O_2^{-\bullet} \rightarrow C_2O_6^{2-} + O_2$$

DISP2:

$$2O_2 + 2e^- \rightarrow 2O_2^{-\bullet}$$

$$O_2^{-\bullet} + CO_2 \rightleftharpoons CO_4^{-\bullet}$$

$$CO_4^{-\bullet} + CO_2 \rightleftharpoons C_2O_6^{-\bullet}$$

$$C_2O_6^{-\bullet} + O_2^{-\bullet} \xrightarrow{k,\text{slow}} C_2O_6^{2-} + O_2$$

In the later two mechanisms, superoxide has a dual role, first as a nucleophile, then as an electron donor. Following a method previously employed by Wadhawan et al.,[9,10] working curves for these three mechanisms were generated according to numerical simulations described by Alden and Compton, using an equal diffusion coefficient assumption.[52] These working curves are shown in Figure 6 and illustrate how the effective number of electrons transferred, N_{eff}, varies as a function of a dimensionless, mechanism-dependent rate constant, K

$$K = \frac{k[O_2]_{bulk}^m r_e^2}{D} \tag{19}$$

where m is a mechanism-dependent parameter and is 0 for ECE or DISP1 processes and 1 for DISP2 processes and k is a first-order rate constant for ECE or DISP 1 and a second-order rate constant for DISP2 processes.[9,10] As noted, in this method, the diffusion coefficients of the neutral and charged species are assumed to be equal. Although the diffusion coefficients of oxygen and superoxide in [EMIM][N(Tf)$_2$] are not identical, this method, nevertheless, proved to be suitable for values that fall within the same order of magnitude.

TABLE 2: Comparison of the Rate Constants for the Reaction of Superoxide with Carbon Dioxide in Aprotic Media

	DMSO[a]	DMF[a]	MeCN[a]	[EMIM][N(Tf)$_2$]
DISP1, k/M^{-1} s^{-1}	4.0×10^5	1.1×10^3	2.8×10^2	1.4×10^3

[a] Data taken from ref 10.

From the experimental data, N_{eff} was deduced by normalizing currents recorded in the presence of carbon dioxide to the current observed for the one electron reduction of oxygen

$$N_{eff} = \frac{i_{lim}^{obs}}{i_{lim}^{1e^-}} \tag{20}$$

Comparison of these values to the working curves generated for the three different mechanisms allowed for the determination of a rate constant for each process. This calculated rate constant, k, is dependent on the carbon dioxide concentration

$$k = \bar{k}[CO_2]^n \tag{21}$$

where $\bar{k}$ is the true rate constant for the reaction and n is the order of the rate-limiting step with respect to carbon dioxide. If eq 13 is rate-limiting, the reaction between superoxide and carbon dioxide would exhibit first-order kinetics with respect to [CO$_2$], indicating an ECE or DISP1 mechanism. Second-order kinetics would be consistent with a DISP2 mechanism and would suggest that either eq 14 or 15 is rate limiting.[9,10]

A value for the solubility of CO$_2$ in [BMIM][PF$_6$] previously reported by Anthony et al.[32] was used to compare how log (k) depends on log [CO$_2$] for the three different mechanisms. The best fit was observed for a DISP1 mechanism, suggesting that eq 13 is the rate-limiting step in the reaction of superoxide with carbon dioxide. The average value of the rate constant was found to be $1.4 \pm 0.4 \times 10^3$ M^{-1} s^{-1} for a DISP1 mechanism. Table 2 shows the values of the rate constants previously determined by Wadhawan et al.[10] for a DISP1 mechanism in various aprotic media.

It has been suggested that, providing the size of the working microelectrode was substantially small enough, the kinetics of the reaction between superoxide and carbon dioxide could be out run, thus enabling simultaneous detection of oxygen and carbon dioxide, a significant advantage for gas sensing applications.[8,9] If such conditions were met, the diffusional loss of superoxide from the electrode−electrolyte interface would be faster than the kinetics of reactions 13−15, allowing for independent signals of O$_2$ and CO$_2$ to be observed. From the determined rate constants, we can estimate the electrode size that would be required to out run the titration reaction between superoxide and carbon dioxide at the working electrode surface.[9,10] Assuming N_{eff} is 1.05 for the one electron reduction of oxygen and that the ionic liquid is saturated with carbon dioxide, the dimensionless rate constant K, as defined above, can be deduced from the working curves for the different mechanisms. This value of K is then used to estimate the radius of the electrode according to the following equation:

$$r = \sqrt{\frac{KD_{O_2}}{k}} \tag{22}$$

Given the rate constants determined for a DISP1 mechanism,

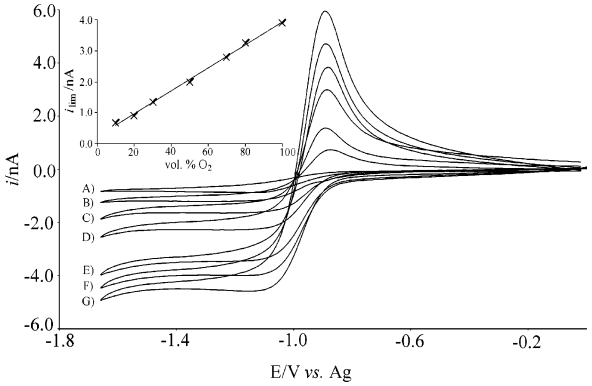

Figure 7. Cyclic voltammograms (1 V s^{-1} scan rate) for the reduction of O_2 in $[N_{6222}][N(Tf)_2]$ at a 10.8 μm Au microdisk electrode at varying vol. % O_2. (A) 10, (B) 20, (C) 30, (D) 50, (E) 70, (F) 80, and (G) 90 vol. % O_2. The inset shows a plot of limiting current vs vol. % O_2.

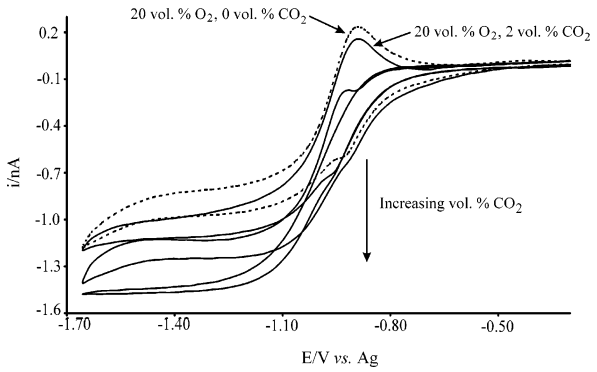

Figure 8. Cyclic voltammograms (200 mV s^{-1} scan rate) for the reduction of O_2 in $[N_{6222}][N(Tf)_2]$ at a 10.8 μm Au microdisk electrode in the presence of increasing amounts of CO_2. The voltammogram for the reduction of O_2 alone is also shown.

an electrode radius of 300 nm would be required in order to out run the kinetics of the reaction between superoxide and carbon dioxide in the ionic liquid, $[EMIM][N(Tf)_2]$.

The reduction of oxygen was next investigated in $[N_{6222}][N(Tf)_2]$. In addition to having a much wider cathodic potential window due to the enhanced stability of the tetraalkylammonium cation, $[N_{6222}][N(Tf)_2]$ is significantly more viscous than $[EMIM][N(Tf)_2]$.[31,53] Consequently, the voltammetry observed in this ionic liquid is notably different. However, analysis of the kinetics via an advanced theory program illustrated that the reaction between superoxide and carbon dioxide proceeded by a similar mechanism to that found for $[EMIM][N(Tf)_2]$.

Reduction of Oxygen of in $[N_{6222}][N(Tf)_2]$. Figure 7 shows the cyclic voltammograms (scan rate 1 V s^{-1}) for the electrochemically reversible reduction of oxygen over the range of 10−100 volume percent at a 10.8 μm (diameter) Au microdisk electrode in $[N_{6222}][N(Tf)_2]$, with a half-wave potential at −0.85 V vs Ag. Nitrogen made up the remainder of the gas mixture. The positive shift of the reduction potential is most likely due to an increase in the solvating properties of $[N_{6222}][N(Tf)_2]$ as compared to $[EMIM][N(Tf)_2]$.[30] The plot of current versus percent volume of O_2 (see inset, Figure 7) shows good linearity for the signal observed for the one electron reduction.

There is a significant discrepancy in diffusion coefficients between the neutral and charged species in this ionic liquid, as illustrated by the *exaggerated* difference in heights of the forward and back peaks. This observation is attributed to the increased viscosity of the tetraalkylammonium salt compared to the imidazolium salt (η = 220 cP and η = 32.1 cP, respectively).[31,53] The structural differences in the cationic components of $[EMIM][N(Tf)_2]$ and $[N_{6222}][N(Tf)_2]$ have significant implications on the potential window as well as the viscosity of the ionic liquid.[26,54] The greater stability of the tetraalkylammonium cation affords a much wider cathodic potential window[27] and the increased alkyl chain length is most likely responsible for the higher viscosity, due to increased van der Waals interactions.[26,54]

The diffusion coefficients of oxygen and superoxide in this ionic liquid were determined as described above for $[EMIM][N(Tf)_2]$ and have been previously reported as $D_{O_2} = 1.48 \pm 0.16 \times 10^{-10}$ m^2 s^{-1} and $D_{O_2^{-\bullet}} = 4.7 \pm 0.5 \times 10^{-12}$ m^2 s^{-1}.[49] The concentration of oxygen was found to be 11.6 mM, more than three times greater than in $[EMIM][N(Tf)_2]$.

Reduction of Carbon Dioxide of in $[N_{6222}][N(Tf)_2]$. The reduction of CO_2 in $[N_{6222}][N(Tf)_2]$ was also investigated by cyclic voltammetry at a gold microdisk electrode over the range of 30−85 vol. % CO_2, with nitrogen making up the remainder of the gas mixture. Good linearity is observed over the detection range (figure not shown). Using the same method as employed for oxygen, the concentration of CO_2 in a saturated sample of $[N_{6222}][N(Tf)_2]$ was determined to be 55.2 mM and the diffusion coefficient was found to be $D_{CO_2} = 2.3 \times 10^{-10}$ m^2 s^{-1}.

The reduction of oxygen in the presence of carbon dioxide was then studied in this ionic liquid and the kinetics of the reaction between superoxide and carbon dioxide analyzed. Given the significant difference in diffusion coefficients of oxygen and superoxide in $[N_{6222}][N(Tf)_2]$, the analytical method employed for $[EMIM][N(Tf)_2]$ was inadequate for this system. A theory and simulation program was required to analyze the kinetics of the reaction in $[N_{6222}][N(Tf)_2]$.

Reduction of Oxygen in the Presence of Carbon Dioxide in $[N_{6222}][N(Tf)_2]$; Kinetic Analysis of the Reaction Between Superoxide and Carbon Dioxide. Cyclic voltammetry also shows an increase in the reductive current and a diminishing of the oxidative back peak for the reduction of oxygen in the presence of CO_2 in $[N_{6222}][N(Tf)_2]$. Figure 8 shows voltammograms (scan rate 0.2 V s^{-1}) for the reduction of 20 vol. % oxygen in the presence of increasing vol. % CO_2. The kinetics of the reaction between superoxide and carbon dioxide in $[N_{6222}][N(Tf)_2]$ were preliminarily analyzed using the same method as employed for $[EMIM][N(Tf)_2]$. However, as this method assumes relatively equal values of the diffusion coefficients of the neutral and charged species,[52] it was not applicable to this more viscous system. Owing to the significant difference in the diffusion coefficients of oxygen and superoxide in this ionic liquid and the fact that nucleophillic attack of CO_2 occurs via the superoxide anion radical, the slow diffusion of $O_2^{-\bullet}$ and of $CO_4^{-\bullet}$, the resulting reaction products, needed to be considered. To this end, a theory and simulation program, as described in the theory section above, was created to enable us to investigate the kinetics of this reaction in $[N_{6222}][N(Tf)_2]$. The experimental data were fit by manual adjustment of the kinetic parameters. This developed theory program was employed to simulate a set of voltammograms recorded for the reduction of a fixed amount of O_2 in the presence of increasing amounts of CO_2 in $[N_{6222}][N(Tf)_2]$ and allowed for the determination of averaged values of α (0.4) and k_0 (2.3×10^{-3} cm s^{-1}), while confirming previously determined values of diffusion coefficients for oxygen and superoxide.[49] Table 3 reports the experimental N_{eff} values as well as the rate constant values obtained by fitting the forward peak of simulated voltammograms to the experimental CVs over a range of carbon dioxide concentrations. The reaction of superoxide with carbon dioxide was found to be the rate-limiting step, indicating the mechanism exhibits first-order kinetics with respect to both superoxide and carbon

TABLE 3: Values of the Rate Constants Obtained from Fitting the Experimental Data for the Reduction of Oxygen in the Presence of Increasing Carbon Dioxide in $[N_{6222}][N(Tf)_2]$

% vol. CO_2	N_{eff}	$k/M^{-1}s^{-1}$
1	1.14	2.0×10^6
2	1.20	1.9×10^6
4	1.29	2.0×10^6
8	1.35	1.8×10^6
16	1.41	0.9×10^6

dioxide. A value of $1.72 \pm 0.45 \times 10^3$ M^{-1} s^{-1} was obtained for the overall second-order rate constant. Although the exact mechanism cannot be determined by this program, these results indicate that the reaction proceeds by either an ECE or DISP1 mechanism, which is similar to that determined by independent kinetic analysis in $[EMIM][N(Tf)_2]$, as discussed previously.

Conclusion

The reduction of oxygen in the presence of carbon dioxide has been investigated by cyclic voltammetry at a gold microdisk electrode in the two room-temperature ionic liquids 1-ethyl-3-methylimidazolium bis(trifluoromethylsulfonyl)imide ($[EMIM][N(Tf)_2]$) and hexyltriethylammonium bis(trifluoromethylsulfonyl)-imide ($[N_{6222}][N(Tf)_2]$). Cyclic voltammetry shows an increase in the reductive wave and the diminishing of the oxidative wave in the presence of CO_2, indicating that the generated superoxide rapidly reacts with carbon dioxide. The kinetics of the reaction between superoxide and carbon dioxide were investigated. A DISP1 mechanism was shown to be the best fit for the reaction in $[EMIM][N(Tf)_2]$, with an overall second-order rate constant of $1.4 \pm 0.4 \times 10^3$ M^{-1} s^{-1}. Although the higher viscosity of $[N_{6222}][N(Tf)_2]$ required an advanced theory and simulation program, the reaction of superoxide with carbon dioxide was found to proceed via a similar mechanism with an overall second-order rate constant of $1.72 \pm 0.45 \times 10^3$ M^{-1} s^{-1}.

Acknowledgment. M.C.B. thanks the Analytical Division of The Royal Society of Chemistry for a studentship and Alphasense Ltd. for CASE funding. O.V.K. thanks the Clarendon fund for partial support. J.D.W. thanks the EPSRC for a studentship. The authors thank Dr. C.E.W. Hahn for loan of the triple-gas mixing pump.

References and Notes

(1) Clark, L. C. *Trans. Am. Soc. Artif. Intern. Organs* **1956**, *2*, 41.
(2) Sawyer, D. T.; Roberts, J. L., Jr. *J. Electroanal. Chem.* **1966**, *12*, 90.
(3) Fujinaga, T.; Izutsu, K.; Adachi, T. *Bull. Chem. Soc. Jpn.* **1969**, *42*, 140.
(4) Lund, W.; Peover, M. E. *J. Electroanal. Chem.* **1970**, *25*, 19.
(5) Albery, W. J.; Barron, P. *J. Electroanal. Chem.* **1982**, *79*.
(6) Hahn, C. E. W. *Clin. Phys. Physiol. Meas.* **1987**, *8*, 3.
(7) Hahn, C. E. W. *Analyst* **1988**, *123*, 57R.
(8) Hahn, C. E. W.; McPeak, H.; Bond, A. M.; Clark, D. *J. Electroanal. Chem.* **1995**, *393*, 61.
(9) Wadhawan, J. D.; Welford, P. J.; Maisonhaute, E.; Climent, V.; Lawrence, N. S.; Compton, R. G.; McPeak, H.; Hahn, C. E. W. *J. Phys. Chem. B* **2001**, *105*, 10659.
(10) Wadhawan, J. D.; Welford, P. J.; McPeak, H. B.; Hahn, C. E. W.; Compton, R. G. *Sens. Actuators B* **2003**, *88*, 40.
(11) Merritt, M. V.; Sawyer, D. T. *J. Org. Chem.* **1970**, *35*, 2157.
(12) Singh, M.; Misra, R. A. *Synthesis* **1989**, 403.
(13) Monte, W. T.; Baizer, M. M.; Little, R. D. *J. Org. Chem.* **1983**, *48*, 803.
(14) Singh, M.; Krishna, N.; Singh, S. D.; Misra, R. A. *Synthesis* **1991**, 291.
(15) Roberts, J. L., Jr.; Calderwood, T. S.; Sawyer, D. T. *J. Am. Chem. Soc.* **1984**, *106*, 4667.
(16) Casadei, M. A. *Eur. J. Org. Chem.* **2001**, 1689.
(17) Casadei, M. A.; Cesa, S.; Feroci, M.; Inesi, A.; Rossi, L.; Moracci, F. M. *Tetrahedron* **1997**, *53*, 167.
(18) Casadei, M. A.; Cesa, S.; Moracci, F. M. *J. Org. Chem.* **1996**, *61*, 380.
(19) Hahn, C. E. W. *Analyst* **1998**, *123*, 57R.
(20) Compton, R. G.; Hahn, C. E. W.; Wadhawan, J. D.; Welford, P. J. *Determining Gas Concentration*; Isis Innovation Limited: U.K., 2003.
(21) Albery, W. J.; Clark, D.; Drummond, H. J. J.; Coombs, A. J. M.; Young, W. K.; Hahn, C. E. W. *J. Electroanal. Chem.* **1992**, *340*, 99.
(22) Hahn, C. E. W.; McPeak, H.; Bond, A. M. *J. Electroanal. Chem.* **1995**, *393*, 69.
(23) Zhou, Z.-B.; Liu, W.-J.; Liu, C.-C. *Sens. Actuators B* **1998**, *52*, 219.
(24) Zhou, Z.-B.; Liu, W.-J.; Liu, C.-C. *Sens. Actuators B* **2000**, *65*, 35.
(25) Carter, M. T.; Hussey, C. L.; Strubinger, S. K. D.; Osteryoung, R. A. *Inorg. Chem.* **1991**, *30*, 1149.
(26) Bonhôte, P.; A., D.; Papageorgiou, N.; Kalyanasundaram, K.; Gratzel, M. *Inorg. Chem.* **1996**, *35*, 1168.
(27) Sun, J.; Forsyth, M.; MacFarlane, D. R. *J. Phys. Chem. B* **1998**, *102*, 8858.
(28) Blanchard, L. A.; Gu, Z.; Brennecke, J. F. *J. Phys. Chem. B* **2001**, *105*, 2437.
(29) Anthony, J. L.; Maginn, E. J.; Brennecke, J. F. *J. Phys. Chem. B* **2001**, *105*, 10942.
(30) AlNashef, I. M.; Leonard, M. L.; Kittle, M. C.; Matthews, M. A.; Weidner, J. W. *Electrochem. Solid-State Lett.* **2001**, *4*, D16.
(31) Hardacre, C.; Holbrey, J. D.; Katdare, S. P.; Seddon, K. R. *Green Chem.* **2002**, *4*, 143.
(32) Anthony, J. L.; Maginn, E. J.; Brennecke, J. F. *J. Phys. Chem. B* **2002**, *106*, 7315.
(33) AlNashef, I. M.; Leonard, M. L.; Matthews, M. A.; Weidner, J. W. *Ind. Eng. Chem. Res* **2002**, *41*, 4475.
(34) Scurto, A., M.; Aki, S., N. V. K.; Brennecke, J. F. *Chem. Commun.* **2003**, 572.
(35) Husson-Borg, P.; Majer, V.; Gomes, M. F. C. *J. Chem. Eng. Data* **2003**, *48* (3), 480-485.
(36) Welton, T. *Chem. Rev.* **1999**, *99*, 2071.
(37) Seddon, K. R. *J. Chem. Technol. Biotechnol.* **1997**, *68*, 351.
(38) Dupont, J.; DeSouza, R. F.; Suarez, P. A. Z. *Chem. Rev.* **2002**, *102*, 3667.
(39) Aoki, K.; Osteryoung, J. *J. Electroanal. Chem.* **1981**, *122*, 19.
(40) Aoki, K.; Osteryoung, J. *J. Electroanal. Chem.* **1984**, *160*, 335.
(41) Welford, P. J.; Brookes, B. A.; Wadhawan, J. D.; McPeak, H. B.; Hahn, C. E. W.; Compton, R. G. *J. Phys. Chem. B* **2001**, *105*, 5253.
(42) Amatore, C.; Fosset, B. *J. Electroanal. Chem.* **1992**, *328*, 21.
(43) Heinze, J. *Electroanalysis* **1981**, *124*, 73.
(44) Heinze, J.; Storzbach, M. *Ber. Bunsen-Ges. Phys. Chem.* **1986**, *90*, 1043.
(45) Svir, I. B.; Klymenko, O. V.; Compton, R. G. *Radiotekhnika* **2001**, *118*, 92.
(46) Stephenson, G. *Mathematical Methods for Science Students*; Prentice Hall: New York, 1973.
(47) Eriksson, K.; Estep, D.; Hansbo, P.; Johnson, C. *Computational Differential Equations*; Cambridge University Press: Cambridge, U.K., 1996.
(48) Klymenko, O. V.; Giovanelli, D.; Lawrence, N. S.; Rees, N. V.; Jiang, L.; Jones, T. G. J. *Electroanalysis* **2003**, *15*, 949.
(49) Buzzeo, M.; Klymenko, O. V.; Wadhawan, J. D.; Hardacre, C.; Seddon, K. R.; Compton, R. G. *J. Phys. Chem. A* **2003**, *107*, 8872.
(50) Bard, A. J.; Faulkner, L. R. *Electrochemical Methods: Fundamentals and Applications*, 2nd ed.; Wiley: New York, 1982.
(51) Sharp, P. *Electrochim. Acta* **1983**, *28*, 301.
(52) Alden, J. A.; Compton, R. G. *J. Phys. Chem. B* **1997**, *101*, 9606.
(53) Evans, R. G.; Klymenko, O. V.; Hardacre, C.; Seddon, K. R.; Compton, R. G. *J. Electroanal. Chem.* **2003**, *556*, 179.
(54) Dzyuba, S. V.; Bartsch, R. *ChemPhysChem* **2002**, *3*, 161.